

Automated contact area measurement on structured surfaces

Ömer C. Küçükyıldız^{1,a)}, Sebastian H. N. Jensen²⁾, Leonardo De Chiffre¹⁾

¹Department of Mechanical Engineering, Technical University of Denmark

²Department of Applied Mathematics and Computer Science, Technical University of Denmark

^aomecak@mek.dtu.dk

Abstract

Structured surfaces involved in a tribological test are quantified using an automated contact area measurement method. The method involves an image segmentation algorithm based on local image gradient extrema. The gradients are then used to accurately determine band-edge segmentation in order to measure the line thickness of the structured surfaces. The traceability of the method was established through an optical standard from NPL in the line-thickness range 10 -100 μm achieving expanded uncertainties in the range 0.5-1.9 μm . The specimen line thickness of different combinations of asperity angle and deformation load, were subject to 10 repeated automatic measurements. The combination of the parameters produce different contact areas, which are interesting for the tribological properties of the surfaces.

Automated measurement, structured surfaces, image segmentation

1. Introduction

In connection with the use of brass specimens featuring structured surfaces in a tribology test, an algorithm was developed for automatic measurement of the contact area by optical means [1]. In this work, the uncertainty estimation of the method is expanded to include the repeatability of the method by carrying out repeated measurements on specimens with varying structured surface. The surfaces are determined by a combination of the initial undeformed asperity angle and the amount of deformation load. The deformation is caused by a simultaneous normal load and a pull transversely to the asperities in a micro-tribotester [2].

2. Method

2.1. Repeated measurements

Structured surfaces with three different asperity angles, each surface containing 10-12 asperities, were produced by milling free cutting brass specimens with a section of 8mm x 8mm. Fig. 1 shows a side view of the surface asperities before deformation while Fig. 2 (left side) shows the surface structure seen from the top after deformation. These specimens were then subjected to three different deformation loads, as shown in table 1.

Table 1. Asperity angles and deformation loads.

Specimen	A	B	C
Asperity angle [°]	90	60	35
Deformation load [kN]	1	2	4

Measurements were carried out on 10 repeated images of each deformed surface captured as single digital photographs using an Alicona optical microscope with a 5x objective magnification and co-axial light illumination. An automated image segmentation algorithm was used in order to quantify the contact line thicknesses. The contact area of the specimen after

deformation is visible on the digital image as 10-12 parallel lines in adequate contrast to the background (fig. 2).

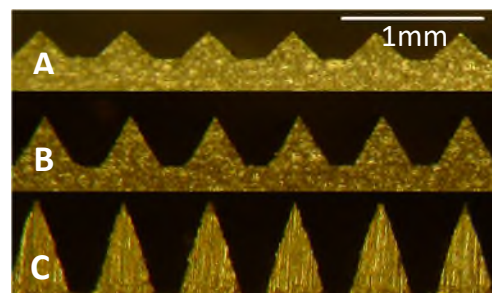


Figure 1. Light optical images of the asperity angles denoted in table 1.

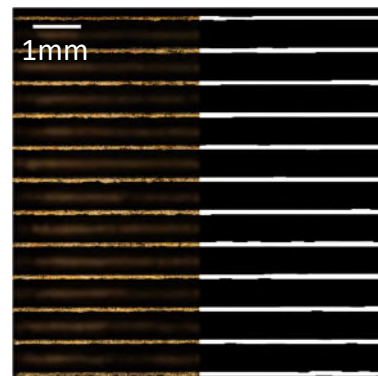


Figure 2. Input image (left) and the segmented image (right) of specimen C. Total dimensions are 8 mm x 8 mm.

2.2. Image segmentation algorithm

The approach to segmentation is simple; the contact surface area is characterized by a strong intensity contrast to the background. Thus, the contact surface edge will be characterized by large magnitude gradients. Additionally the contact lines are safely assumed to be horizontal on the

images, thus the search only takes place along the vertical gradients.

A simple algorithm is devised that finds the upper and lower edge of a contact area via gradient segmentation. The complete area is then segmented as the region between the upper and lower edges. The procedure is described in the following.

Let I be the input image in grayscale, u the upper edge gradient threshold, l the lower edge gradient threshold, S the structuring element and K the maximum contact surface width.

$$I_l = \frac{dl}{dy} < l \quad (1)$$

$$I_u = \frac{du}{dy} > u \quad (2)$$

$$S_u = \mathbf{0}_K \mathbf{1}_{K+1}^T \quad (3)$$

$$S_l = \mathbf{1}_{K+1} \mathbf{0}_K^T \quad (4)$$

The segmented image B is then obtained from the input image I by finding the upper and lower edge of the contact surface via gradient thresholding.

$$B = (I_u \oplus S_u) \cup (I_l \oplus S_l) \quad (5)$$

Then the complete segmentation is produced by growing the edges towards each other (by dilation, \oplus) and taking the union of the grown regions.

A result of automatic segmentation is shown in Fig. 2 (right) compared to the input image of the contact lines (left).

2.3. Uncertainty quantification

The expanded uncertainty ($k=2$) of the imaging and subsequent segmentation was determined on the background of 10 repeated measurements on NPL optical dimensional standard pattern 4U with range 10-100 μm and with calibration uncertainty 0.14 μm [3]. The uncertainty related to the repeated measurements on the three specimens A-C is added to the expanded uncertainty, which is determined according to the GUM [4]:

$$U = k \cdot \sqrt{u_{ref}^2 + u_{rep}^2 + u_{spec}^2 + u_p^2 + u_e^2}$$

where

u_{ref} : uncertainty from reference standard calibration

u_{rep} : uncertainty from repeatability of measurements on the reference standard

u_{spec} : uncertainty from repeatability of measurements on a single line of the specimen

u_p : uncertainty from line width variation across the specimen

u_e : uncertainty from coefficient of thermal expansion of specimen

3. Results

The average of the 10 repeated automated measurements and the expanded uncertainty for each line thickness were calculated for each of the three specimens A-C.

The uncertainty of the measurement result depends on a combination of the uncertainty of the method and the characteristics of the deformed asperity. A large deformation of the asperity leading to burr formation is sensitive to light

conditions between repeated measurements, which increases the uncertainty.

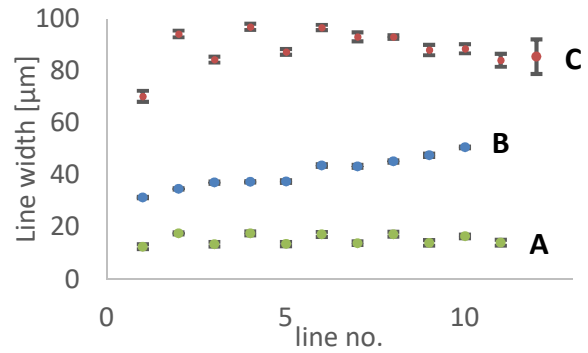


Figure 3. Automatic determination of average line width for specimens A-C. Each symbol represents the average of 10 repeated measurements. Error bars show the expanded measurement uncertainty ($k=2$).

The average line width and average expanded uncertainty for each specimen were calculated and are reported in table 2.

Table 2. Average (Y), standard deviation (STD. Y), expanded uncertainty (U) and relative uncertainty (U/Y) of the repeated measurements.

Specimen	A	B	C
Y [μm]	15.3	40.9	88.5
STD. Y [μm]	0.4	0.2	1.0
U [μm]	0.8	0.5	1.9
U/Y	6%	1%	2%

4. Discussion

Since the line widths of specimen A are small, the uncertainty coming from the calibration artefact is significant. For specimen C the large deformation of the asperity leads to burr formation that is sensitive to slightly changing light conditions between repeated measurements and thus increases the uncertainty. Specimen B is not affected by these errors and yields the lowest uncertainty. Based on the expanded uncertainties, the algorithm appears adequate in quantifying the line thickness for all three types of specimen surfaces.

5. Summary and conclusion

A method for automated measurement of structured surfaces featuring deformed horizontal lines from a digital image by the means of an algorithm has been presented. The procedure of the algorithm and the calculation of the expanded uncertainties of the method on three different surfaces have been exemplified. It was shown that the method is sufficient for quantifying the linewidths of the three examples of structured surfaces.

References

- [1] Küçükıldız Ö C, Jensen S H N and De Chiffre L 2016 Contact area measurements on structured surfaces *Poster presented at Euspen's S.I.G. Meeting, Copenhagen, Denmark*
- [2] Nielsen P S, Paldan N A, Calaan M and Bay N 2011 Scale effects in metal-forming of friction and lubrication *Proceeding of the Institution of Mechanical Engineers, Part J: Journal of Engineering Tribology* **225** 924–931
- [3] <http://www.npl.co.uk/measurement-services/dimensional/optical-dimensional-standard>
- [4] BIPM, Evaluation of measurement data — Guide to the expression of uncertainty in measurement, JCGM 100:2008, GUM 1995 with minor corrections.